Available online at www.sciencedirect.com
SCIENCE DIRECT®
Journal of Organometallic Chemistry 679 (2003) 72–78
Journal of Organometallic Chemistry
www.elsevier.com/locate/jorganchem

Ruthenium cluster compounds containing 1,1′-bis(diphenylphosphino)ferrocene (dppf): an electrochemical analysis and the crystal structure of $[Ru_3(CO)_{11}]_2(\mu\text{-dppf})$☆

Abby R. O'Connor, Chip Nataro *, Arnold L. Rheingold [1]

Department of Chemistry, Lafayette College, Easton, PA 18042, USA
Department of Chemistry & Biochemistry, University of Delaware, Newark, DE 19716, USA

Received 7 May 2003; received in revised form 30 May 2003; accepted 30 May 2003

Abstract

The electrochemistry of 1,1′-bis(diphenylphosphino)ferrocene (dppf) derivatives of $Ru_3(CO)_{12}$ was investigated. Two known compounds $[Ru_3(CO)_8(\mu\text{-dppf})_2$ (**1**) and $Ru_3(CO)_{10}$dppf (**2**)] and a new compound $[Ru_3(CO)_{11}(\mu\text{-dppf})Ru_3(CO)_{11}$ (**3**)] were prepared. Compound **3** was characterized spectroscopically and an X-ray crystal structure was obtained. The reductive electrochemistry of **1** and **2** showed an irreversible reduction and a follow-up oxidation, similar to $Ru_3(CO)_{12}$. The electrochemistry of compound **3** showed two irreversible waves and a follow-up oxidation. A trend in the reduction potential vs. the number of coordinated phosphorus atoms was noted. The oxidative electrochemistry of **1**–**3** showed a dppf-based chemically reversible wave, and an irreversible wave similar to that of $Ru_3(CO)_{12}$. Trends were also noted between the oxidation potential and the number of coordinated phosphorus atoms.

Keywords: Electrochemistry; 1,1′-bis(diphenylphosphino)ferrocene; Crystal structure; Cyclic voltammetry; Synthesis

1. Introduction

1,1′-Bis(diphenylphosphino)ferrocene (dppf) is quite remarkable due to the various coordination modes that it can adopt to match the sterics of the existing molecular environment [1,2]. The most common coordination mode of dppf is bidentate, in which it bonds to one metal in the same structural unit as seen in $M(CO)_4(\eta^2\text{-dppf})$ (M = Cr, Mo, or W) [3]. Compounds are also known where dppf bonds in a unidentate mode leaving an uncoordinated phosphorus atom, for example $M(CO)_5(\eta^1\text{-dppf})$ (M = Cr, Mo, or W) [3]. In cluster compounds dppf can be bonded in a variety of modes such as closed-bridged and open-bridged [1,2]. In the closed-bridge mode, dppf is bonded to two different metals in the same cluster as in $Fe_3(CO)_{10}$(dppf), whereas in the open-bridged mode, dppf is bonded to metals in different clusters as seen in $[Fe_3(CO)_{11}]_2(\mu\text{-dppf})$ [4].

Not only does dppf have a variety of interesting bonding modes, it also displays interesting properties. The primary use of dppf has been as a ligand in catalysis. For example, the dechlorination of highly chlorinated PCB's occurs under mild conditions using $[PdCl_2(\eta^2\text{-dppf})]$ as the catalyst [5]. There are a variety of factors that can influence the catalytic properties of compounds containing dppf, one of which is the redox active ferrocene backbone of dppf [1]. The dppf ligand can enhance the electron transfer properties of the

☆ Presented in part at the 224th National Meeting of the American Chemical Society, Boston, MA, August 18–22, 2002, see: *Abstracts of Papers*, INOR. 388.

* Corresponding author. Tel.: +1-610-330-5216; fax: +1-610-330-5714.
E-mail address: nataroc@lafayette.edu (C. Nataro).
[1] Department of Chemistry and Biochemistry, University of San Diego, La Jolla, CA 92093, USA.

0022-328X/03/$ - see front matter © 2003 Elsevier B.V. All rights reserved.
doi:10.1016/S0022-328X(03)00512-6

catalyst thereby enhancing the activity of the catalyst [6]. By investigating the electronic nature of dppf-containing compounds, the catalytic activity of these compounds can be better understood.

Previous studies have investigated the electrochemical behavior of dppf in a variety of solvents [7–10]. In contrast to the simple one electron oxidation of ferrocene, the electrochemistry of dppf is more complicated. The electrochemistry of a variety of compounds containing dppf has been investigated, however very few of those have been cluster compounds [1]. While electrochemical studies have been performed on two dppf-containing derivatives of $Fe_3(CO)_{12}$ [4], it is somewhat surprising that no derivatives of $Ru_3(CO)_{12}$ have been investigated.

Two derivatives of $Ru_3(CO)_{12}$ containing dppf have been reported [11]. In both compounds, $Ru_3(CO)_8(dppf)_2$ (**1**) and $Ru_3(CO)_{10}$dppf (**2**), dppf acts as a closed bridge ligand to the ruthenium cluster (Fig. 1). We report the synthesis and characterization of a new ruthenium cluster, **3**, which contains an open-bridged dppf ligand linking two Ru_3 units. The molecular structure of the new compound was obtained and compared to related open-bridged ruthenium cluster compounds. Finally, the electrochemistry of compounds **1**–**3** was investigated and compared to $Ru_3(CO)_{12}$, dppf and a series of analogous Fe_3 clusters.

2. Results and discussion

A variety of experimental conditions were explored in an attempt to synthesize compound **3**. In all cases, the signal for free dppf in the ^{31}P-NMR ($\delta = -16.9$ ppm) was monitored to determine when the dppf was consumed. The optimal preparation of **3** employed sodium benzophenone ketyl as the catalyst and did not result in formation of **2**. Compound **3** was purified by column chromatography on silica gel.

A complete spectroscopic study of **3** was performed using NMR. The ^{1}H-NMR of **3** in $CDCl_3$ showed a multiplet for the aryl protons at δ 7.39 and two broad singlets for protons of the monosubstituted cyclopentadienyl rings of dppf. The integral values were in agreement with expected number of protons. The assignment of the carbons was based upon the coupling constants and DEPT data. The ^{13}C–^{1}H HECTOR and ^{1}H–^{1}H COSY aided in the assignment of the protons. A ^{31}P–^{1}H HECTOR was obtained, but was not useful in assigning the aryl protons. The ^{1}H and ^{13}C-NMR data for **2** were in good agreement with prior studies, however the ^{31}P{^{1}H}-NMR spectrum of **2** has not been reported previously [11]. The chemical shifts for **2** and **3** are nearly identical, making it difficult to distinguish the two compounds exclusively by ^{31}P{^{1}H}-NMR.

The iron analogues of **2 (2Fe)** and **3 (3Fe)** have been prepared and characterized by Stein and Fujiwara [4]. The ^{13}C{^{1}H}-NMR data for compounds **3** and **3Fe** are quite similar however, the carbonyl peak of **3Fe** is reported to be a broad singlet due to scrambling of the CO ligands [4]. The ^{31}P{^{1}H}-NMR of **2Fe** is a singlet at 41.5 ppm while **3Fe** is a singlet at 49.3 ppm [4]. The difference of ca. 20 ppm between the Fe and Ru compounds is a reflection of the difference in the electron donating ability of the metal in the cluster. Metals are more electron rich going down a family on the periodic table [12]. It is also common to see a trend of upfield shifts in a series of compounds in which a phosphorus atom is bound to the different metals in a group. For example, the ^{31}P{^{1}H} signal for $(CO)_4M(\eta^2$-dppf) (M = Cr, Mo, or W) shifts further upfield going down the group [3]. Compared to the ruthenium analogs, **2Fe** and **3Fe** have a greater difference in chemical shift, ca. 8 ppm, making identification of each species by ^{31}P-NMR easier. The IR spectra of the iron compounds were significantly different from the related ruthenium compounds. The iron analogues showed an IR band around 1790 cm^{-1} which was assigned to bridging carbonyl ligands [4]. There is not a band that could be attributed to a bridging carbonyl in the IR spectrum of **2** [11] or **3**. This is not surprising as bridging carbonyls are observed in $Fe_3(CO)_{12}$, but not in $Ru_3(CO)_{12}$ [13].

Additional support for the lack of bridging carbonyls can be seen in the crystal structures of **2** [11] and **3** (Fig. 2). The dppf ligand in **3**, adopts an antiperiplanar geometry, which is defined as having a τ angle of 180° [1,2]. The phosphorus atoms lie out of the cyclopentadienyl plane on the side away from the iron center, as anticipated for dppf in an open-bridging mode [1,2]. Select bond distances and angles are listed in Table 1.

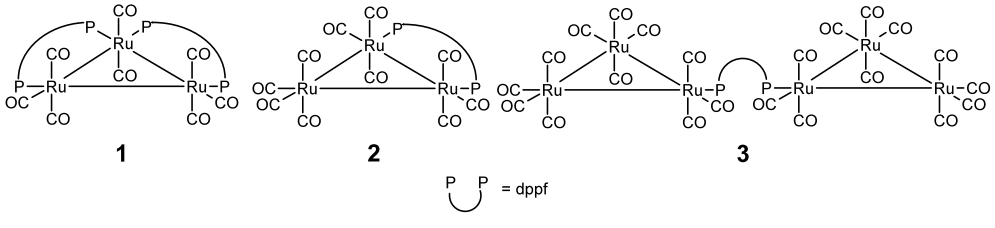

Fig. 1. Derivatives of $Ru_3(CO)_{12}$ containing dppf.

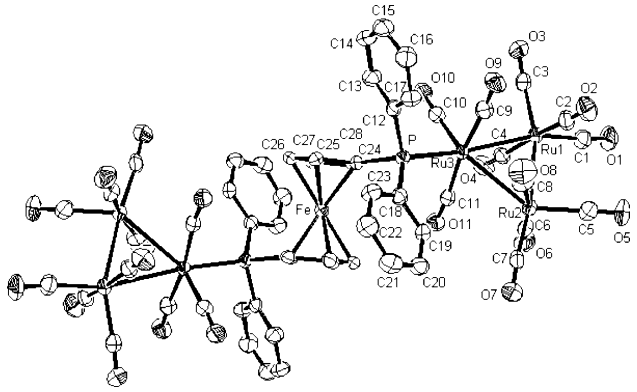

Fig. 2. ORTEP of the molecular structure of **3**.

Table 1
Select bond lengths (Å) and angles (°) for $[Ru_3(CO)_{11}]_2(\mu\text{-dppf})$, **3**

Bond distances			
$Ru_1–Ru_3$	2.8459(7)	$Ru_1–C_{eq}$ (avg.)	1.925
$Ru_2–Ru_3$	2.8980(7)	$Ru_2–C_{eq}$ (avg.)	1.931
$Ru_1–Ru_2$	2.8491(8)	$Ru_3–C_{eq}$	1.871(6)
Fe–C (avg.)	2.045	$C_{ax}–O$ (Ru_1 & Ru_2 avg.)	1.140
$Ru_3–P$	2.3529(16)	$C_{ax}–O$ (Ru_3 avg.)	1.144
P–P	7.161 [a]	$C_{eq}–O$ (Ru_1 & Ru_2 avg.)	1.122
$Ru_1–C_{ax}$ (avg.)	1.943	$C_{eq}–O$ (Ru_3)	1.149(7)
$Ru_2–C_{ax}$ (avg.)	1.942	Avg. δ_P [b]	−0.260 [a]
$Ru_3–C_{ax}$ (avg.)	1.931		
Bond angles			
$Ru_3–Ru_1–Ru_2$	61.176(17)	*cis*-$C–Ru_1–C$ (avg.)	93.98
$Ru_1–Ru_2–Ru_3$	59.359(17)	$C_4–Ru_1–C_2$	170.4(3)
$Ru_1–Ru_3–Ru_2$	59.465(19)	*cis*-$C–Ru_2–C$ (avg.)	94.14
$O–C–Ru_1$ (avg.)	174.99	$C_8–Ru_2–C_6$	169.1(3)
$O–C–Ru_2$ (avg.)	175.85	*cis*-$C–Ru_3–C$ (avg.)	94.36
$O–C–Ru_3$ (avg.)	175.26	$C_{11}–Ru_3–C_9$	170.6(3)
P–Fe–P	180.0 [a]	Cent.–Fe–Cent.	179.97 [a]
τ [c]	180.0 [a]	θ [d]	0.0 [a]
C–Ru–Ru–C (avg.)	33.4		

[a] Calculated using ORTEP-3 for Windows Ref. [28].
[b] Deviation of the P atom from the Cp plane, a positive value meaning the P is closer to the Fe.
[c] The torsion angle $C_A–X_A–X_B–C_B$, where C is the carbon bonded to the P and X is the centroid.
[d] The dihedral angle between the two Cp rings.

The open-bridging bonding mode of dppf observed in compound **3** has similar bonding characteristics to other open-bridged ruthenium clusters. The Ru–P distance in **3** is comparable to those found in the related structures $[Ru_3(CO)_{11}]_2$dppe (2.345(2) Å) and $[Ru_3(CO)_{11})]_2$dppbz (2.357(3) Å where dppbz = 1,4-bis(diphenylphosphino)benzene) [14]. The Ru–Ru bond *cis*- to the phosphorus atom in **3** is the longest Ru–Ru bond. This feature has been noted in other $Ru_3(CO)_{12}$ derivatives such as $Ru_3(CO)_{11}(PFcPh_2)$ [11], $[Ru_3(CO)_{11}]_2$dppe [14] and $[Ru_3(CO)_{11})]_2$dppbz [14]. In addition, the axial (out of the Ru_3 plane) Ru–C bonds of **3** are slightly longer than the equatorial (in the Ru_3 plane) Ru–C bonds; a similar pattern was observed in $Ru_3(CO)_{11}(PFcPh_2)$ [11], $[Ru_3(CO)_{11}]_2$dppe [14] and $[Ru_3(CO)_{11})]_2$dppbz [14]. A noteworthy difference is that there is significant twisting of the Ru_3 cluster in compound **3** as noted in the average C–Ru–Ru–C torsion angle of 33.4°. This is substantially larger than the analogous torsion angles in $Ru_3(CO)_{12}$ (1.78°) [15], $Ru_3(CO)_{11}(PFcPh_2)$ (13.1°) [11] and $Ru_3(CO)_{10}$dppf (28.4°) [11]. This twist does not appear to be a function of chelate phosphines in an open-bridging coordination mode as the average torsion angles in $[Ru_3(CO)_{11}]_2$dppe and $[Ru_3(CO)_{11})]_2$dppbz are ca. 3.4° [14]. The only other monophosphine derivative of $Ru_3(CO)_{12}$ with an average torsion angle similar to **3** is $Ru_3(CO)_{11}[(\eta^1{:}\eta^5\text{-}C_2P^t_3Bu_2)FeCp^*]$ (32.4°) [16]. It is unclear why dppf causes such an extreme distortion of the Ru_3 core in **3**. It does not appear to be due to the ferrocenyl group as the average torsion angle in $Ru_3(CO)_{11}(PFcPh_2)$ (13.1°) [11] is only slightly larger than that of $Ru_3(CO)_{11}(PPh_3)$ which is 8.38° [17].

Cyclic voltammetry was used to determine the reduction and oxidation potentials for compounds **1**–**3** and ruthenium dodecacarbonyl. The decamethylferrocene/decamethylferrocenium couple was used as a standard for all measurements taken. This choice was made instead of using the more typical ferrocene/ferrocenium couple because the compounds showed waves at potentials similar to ferrocene, which would make it difficult to distinguish the response of the compounds. The standard potential difference of 0.55 V for $Fc^{*0/+}$ vs. $Fc^{0/+}$ was then used to establish the potentials of the ruthenium cluster compounds relative to ferrocene [18].

The electrochemistry of dppf and $Ru_3(CO)_{12}$ has been studied using a variety of conditions. There is no reductive electrochemistry of dppf in DCM. There is an oxidative wave at 0.23 V vs. $Fc^{0/+}$ however, unlike ferrocene, it is not a simple one-electron process [10]. The oxidative and reductive electrochemistry of $Ru_3(CO)_{12}$ has also been studied in DCM. The reduction of $Ru_3(CO)_{12}$ occurs at ca. −1.44 V vs. $Fc^{0/+}$ [19]; it is a two-electron process, which leads to cleavage of an Ru–Ru bond and formation of $Ru_3(CO)_{12}^{2-}$ [21]. Upon reversing the scan, an irreversible anodic wave is observed. The nature of this oxidation has received considerable attention, and a thorough investigation by Rieger determined that this wave is due to oxidation of the initially formed dianion [22]. In DCM, the potential of this wave is highly dependent on the coordinating ability of the supporting electrolyte anion. For example, the anodic wave occurs at −0.89 V in $NBu_4^+ClO_4^-$ [19] as compared to −0.50 V in PPN^+OAc^- [19] and this difference is attributed to coordination of the acetate anion [21]. Our results for the reduction of $Ru_3(CO)_{12}$ in DCM with $NBu_4^+PF_6^-$ supporting electrolyte are consistent with other non-coordinating anions (Table 2). In

Table 2
Oxidation and reduction potentials for $Ru_3(CO)_{12}$ and compounds **1**–**3**

Compound	Oxidation			Reduction		
	E_{pa}	E_{pa}	E_{pc}	E_{pc}	E_{pc}	E_{pa}
$Ru_3(CO)_{12}$		0.83		−1.69		−1.17
1	−0.04	0.64	0.50	−2.27		−0.91
2	0.24 [a]	0.70	0.55	−2.05		−1.16
3	0.48	0.74	0.71	−1.87	−2.00	−1.15

1.0mM solution at 295 K, volts vs. $Fc^{0/+}$, in DCM with 0.1 M 1.0 M $Bu_4N^+PF_6^-$, scan rate 100 mV s^{-1}.
[a] $E_{1/2}$ value.

addition, the oxidative electrochemistry of $Ru_3(CO)_{12}$ shows one irreversible wave at ca. 0.98 V [19,21].

The reductive electrochemistry of **1**–**3** is similar to the parent $Ru_3(CO)_{12}$ (Table 2). The compounds display an irreversible cathodic wave at ca. −2 V and, upon reversing the scan, an irreversible anodic wave at ca. −1 V is observed. The exception to this is compound **3**, which exhibits two cathodic waves at scan rates less than 200 mV s^{-1} and one at higher scan rates (Fig. 3). Similar behavior was observed in the reductive electrochemistry of $[Ru_3(CO)_{11}]_2$dppa [23]. The first wave is attributed to reduction of $[Ru_3(CO)_{11}]_2$dppa, and the second is attributed to the reduction of $Ru_3(CO)_{11}(\eta^1$-dppa) which forms as a result of cluster decomposition. A similar result was observed in the reductive electrochemistry of a monodentate phosphine derivative of $Ru_3(CO)_{12}$. The reductive electrochemistry of $Ru_3(CO)_{11}(PPh_3)$ displays two reduction waves, with the second wave being attributed to the reduction of

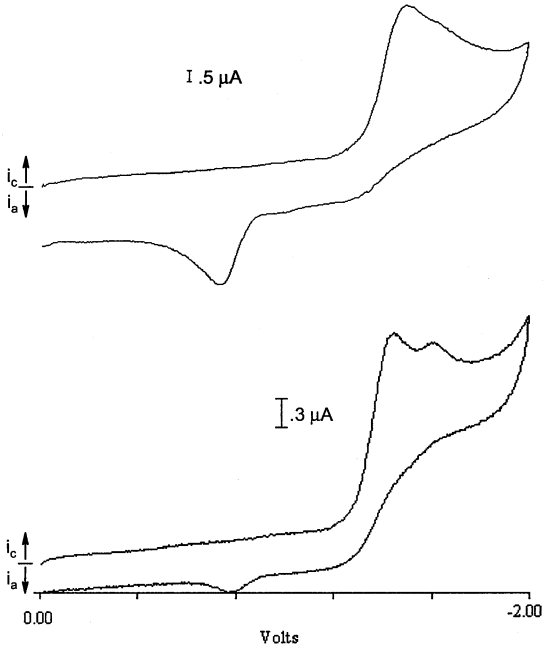

Fig. 3. Reductive CV of **3** at 100 (bottom) and 800 mV s^{-1} (top).

$Ru_3(CO)_{10}(PPh_3)_2$ that is formed as a decomposition product [21]. The second wave for compound **3** occurs at a very similar potential to that observed for compound **2**. In addition, we have not detected the formation of $Ru_3(CO)_{11}(\eta^1$-dppf) during any of our syntheses. Therefore, the second wave observed in the reduction of **3** is likely due to the formation of **2** as opposed to formation of the unidentate species, $Ru_3(CO)_{11}(\eta^1$-dppf).

The reductive electrochemistry of **2** and **3** can be compared to the analogous iron clusters. The reductive electrochemistry of **2Fe** displays two cathodic waves and one anodic return wave in DCE. At a scan rate of 200 mV s^{-1} on a Pt working electrode the reduction potentials for **2Fe** are −1.48 and −1.81 V with a follow-up wave at −1.01 V [4]. The original study references the potentials vs. SCE, however they are presented here vs. $Fc^{0/+}$ by adding −0.59 V to the reported potentials [24]. The first wave is assigned to the formation of $[Fe(CO)_{10}(dppf)]^-$, and the second is attributed to $[Fe(CO)_{10}(dppf)]^{-2}$ [4]. The analogous ruthenium compound, **2**, displays a single reduction at a potential significantly more negative than that of **2Fe**. This indicates that the ruthenium compound is harder to reduce as expected, since ruthenium is more electron rich than iron [25]. This same pattern is seen in the $M_3(CO)_{12}$ (M = Fe or Ru) clusters, where the ruthenium cluster has a significantly more negative reduction potential than the iron analogue [26]. Compound **3Fe** shows a similar pattern to that observed for **3**. There are two chemically irreversible cathodic waves at −1.40 and −1.92 V and a follow-up at −0.94 V [4]. The first wave is a two electron reduction to $[Fe_3(CO)_{11}]_2dppf^{-2}$ and the second is the reduction of an uncharacterized decomposition product, presumably **2Fe**. Again, the reduction of the ruthenium cluster occurs at a significantly more negative potential.

As more carbonyl ligands on the cluster are exchanged for phosphine ligands, the reduction potentials become more negative. To gauge this effect, the reduction potentials of the clusters were plotted against the ratio of the number of phosphorus atoms in the compound to the number of ruthenium atoms in the compound and a good correlation was obtained (R^2 = 0.982). Since phosphines are more electron donating than carbonyls [12], this general trend was anticipated. A similar trend is noted in the series $Ru_3(CO)_{12-n}(PPh_3)_n$ (n = 1, 2 or 3) where the reduction potentials are −1.44 V for $Ru_3(CO)_{12}$, −1.68 V for n = 1, −1.75 V for n = 2 and −2.04 V for n = 3 [19,21].

The oxidative electrochemistry of $Ru_3(CO)_{12}$ in DCM displays an irreversible wave at 0.98 V [19,21]. It should be noted that after each trial the electrode needed to be repolished due to significant amounts of material adhering to the electrode. The phosphine derivatives, $Ru_3(CO)_{12-n}(PPh_3)_n$ (n = 1, 2, or 3), display oxidation waves that become less positive as n increases suggesting

that the cluster becomes more electron rich as phosphine ligands are added [21]. There are two waves observed in the oxidative electrochemistry of compounds **1**–**3** (Table 2). The first wave is attributed to the oxidation of the dppf ligand, and the second to the oxidation of the ruthenium cluster. The dppf-based wave is irreversible for compounds **1** and **3**, and reversible for compound **2**. The cluster-based waves appear to be irreversible, however there is a small cathodic wave observed upon reversing the scan. The oxidation potentials are sensitive to the chemical environment. Compound **1**, which has the highest ratio of phosphorus to ruthenium, displays the lowest oxidation potentials while $Ru_3(CO)_{12}$ is the highest. There is a good correlation between both the dppf-based and cluster-based oxidation potentials and the phosphorus to ruthenium ratio ($R^2 = 0.979$ and 0.923, respectively). Unfortunately, the oxidative electrochemistry of **2Fe** and **3Fe** was not reported.

The average IR value for the carbonyls of a compound can be used as an estimate of the electron density at a metal center [27]. This can also serve to predict the redox properties of a series of compounds. The average ν_{CO} for **2** is 1992 cm^{-1} and for **1** it is 1981 cm^{-1} [11]. The average IR values shift to lower wavenumbers when more phosphorus atoms, relative to the amount of ruthenium atoms, are present. There is excellent correlation between the average ν_{CO} for compounds **1**–**3** and the oxidation and the reduction potentials for these compounds ($R^2 = 0.9999$ for the dppf-based oxidation, 0.9998 for the cluster-based oxidation and 0.983 for the reduction).

3. Conclusion

The compound $[Ru_3(CO)_{11}]_2$(μ-dppf), **3**, was prepared by reaction of $Ru_3(CO)_{12}$ and dppf using sodium benzophenone ketyl catalyst. Compound **3** has been characterized by IR and NMR spectroscopy. The ^{31}P-NMR for both **2** and **3** are reported and are found at similar chemical shifts, making it difficult to distinguish **2** from **3** solely on this information. The crystal structure of **3** was determined and compared with other triruthenium cluster compounds. The electrochemical properties of these dppf containing cluster compounds were investigated and compared to the parent cluster, $Ru_3(CO)_{12}$, PPh_3 derivatives of $Ru_3(CO)_{12}$ and iron analogues. In general, the ruthenium cluster becomes harder to reduce and easier to oxidize upon the addition of more phosphorus ligands. There is also excellent correlation between the redox potentials and the average ν_{CO} values.

4. Experimental

4.1. General procedures

All preparative reactions and purifications were carried out under an atmosphere of argon using standard Schlenk techniques. Solvents were purified under nitrogen using standard methods. Hexanes and DCM were distilled from CaH_2 under argon. Tetrahydrofuran (THF) was distilled over potassium benzophenone ketyl. Separation of products was achieved by column chromatography on silica gel using mixtures of hexanes–DCM as the eluent. The NMR data were obtained in $CDCl_3$ on a JEOL Eclipse 400 FT-NMR. The internal standard for ^{1}H and ^{13}C-NMR was TMS ($\delta = 0.00$ ppm) while for the $^{31}P\{^1H\}$-NMR, 85% H_3PO_4 was used as an external reference. Infrared spectra, with CH_2Cl_2 as the solvent, were obtained on a Mattson Satellite FT-IR spectrophotometer using sodium chloride plates. Elemental analysis was performed by Quantitative Technologies, Inc.

Triruthenium dodecacarbonyl ($Ru_3(CO)_{12}$), ferrocene, decamethylferrocene, and dppf were purchased from Strem. Ferrocene was sublimed prior to use. Compounds **1** and **2** were prepared according to the literature procedures [11]. The ^{31}P-NMR of compound **2** has not been reported; it occurs as a singlet at 27.4 ppm in $CDCl_3$. Tetrabutylammonium hexaflurophosphate ($Bu_4N^+PF_6^-$) was purchased from Aldrich and dried in vacuo prior to use.

4.2. Synthesis

THF (6.0 ml) was added to $Ru_3(CO)_{12}$ (100.0 mg, 0.16 mmol) and allowed to stir for 10 min, until dissolved, at which point dppf (40.0 mg, 0.072 mmol) was added. A sodium benzophenone ketyl solution in THF (10 ml, 0.025 M) was prepared and added dropwise to the solution, which quickly changed color from orange to dark red. The reaction was stirred for 10 min and then the solvent was removed in vacuo. The solid residue was dissolved in a mixture of hexanes and methylene chloride and purified by column chromatography on silica gel (height 8 in. diameter 1 in.). Two identifiable bands were obtained off of the column. The first band eluted with hexanes and was identified by IR as $Ru_3(CO)_{12}$ and recovered (33.0 mg, 0.052 mmol). The second band was dark red and eluted with hexanes–DCM (1:1 v/v) yielding $[Ru_3(CO)_{11}]_2$(μ-dppf) **(3)** (10.0 mg, 0.0053 mmol, 9.4% yield). **(3)** IR (CH_2Cl_2): ν_{CO} cm^{-1} 2094 (m), 2045 (m), 2014 (s), 1988 (w), 1954 (sh), 1924 (w). ^{1}H ($CDCl_3$): δ 7.39 (m, 20H, -Ph), 4.23 (br s, 4H, H_B), 3.96 (br s, 4H, H_A). $^{13}C\{^1H\}$ ($CDCl_3$): δ 204.1 (s, Ru–*C*O), 136.4 (d, $^1J_{CP} = 46.4$ Hz, C_{ipso}), 132.5 (d, $^2J_{CP} = 12.2$ Hz, C_{ortho}), 130.5 (s, C_{para}), 128.3 (d, $^3J_{CP} = 9.95$, C_{meta}), 81.9 (d, $^1J_{CP} = 47.5$ Hz, C24), 74.5 (d,

$^{2}J_{CP} = 11.1$ Hz, C25 and C28), 73.8 (d, $^{3}J_{CP} = 6.63$, C26 and C27). $^{31}P\{^{1}H\}$ ($CDCl_3$): δ 27.6 (s). Anal. Calc. for $C_{56}H_{28}FeO_{22}P_2Ru_6$ $1.5CH_2Cl_2$: C, 36.26; H, 1.64. Found: C, 36.21; H, 1.90.

4.3. X-ray crystallography

Crystals of **3** were obtained by slow evaporation of the hexanes–DCM solution obtained from the column. This yielded small, needle-like crystals that were dark red. Crystallographic data are presented in Tables 1 and 3. The data were collected on a Bruker platform system with an APEX CCD detector. Data were corrected for absorption using the SADABS program. The space group was unambiguously assigned from the diffraction data. The structure was solved by heavy-atom methods and refined with all non-hydrogen atoms anisotropic and hydrogen atoms in idealized locations. All routines and software are contained in the current Bruker and SHELXL packages (Bruker AXS, Madison, WI).

Table 3
Crystal data and structure refinement for $[Ru_3(CO)_{11}]_2$-$[(PPh_2C_5H_4)_2Fe]$

Formula	$C_{56}H_{28}FeO_{22}P_2Ru_6$
Formula weight	1776.99
Crystal system	Monoclinic
Space group	$P2_1/c$
a (Å)	13.2625(18)
b (Å)	9.7004(13)
c (Å)	22.661(3)
α (°)	90
β (°)	91.483(2)
γ (°)	90
V (Å^3)	2914.4(7)
D_{calc} (g cm^{-3})	2.025
Z, Z'	2, 0.5
$F(0\,0\,0)$	1720
Crystal size (mm)	$0.25 \times 0.25 \times 0.04$
T (K)	153(2)
Wavelength (Å)	0.71073
Absorption coefficient	1.889 mm^{-1}
Theta range for data collection (°)	2.28–28.28
Index ranges	$-17 \le h \le 17$, $-12 \le k \le 11$, $-28 \le l \le 15$
Reflections collected	16 734
Independent reflections	6656 [$R_{int} = 0.0540$]
Completeness to $\theta = 28.28°$	95.1%
Absorption correction	SADABS
Max/min transmission	0.9283 and 0.6495
Refinement method	Full-matrix least-squares on F^2
Data/restraints/parameters	6656/0/394
Goodness-of-fit on F^2	1.173
Final R indices [$I > 2\sigma(I)$]	$R_1 = 0.0546$, $wR^2 = 0.1242$
R indices (all data)	$R_1 = 0.0760$, $wR^2 = 0.1331$
Largest difference peak and hole (e Å^{-3})	2.283 and -1.089

4.4. Electrochemistry

Cyclic voltammetric studies were done with a Princeton Applied Research 263-A potentiostat. The electrochemical potentials were measured and analyzed by Power Suite. Solutions of the analyte were 1.0 mM in 10.0 ml of DCM, and contained 0.1 M $Bu_4N^+PF_6^-$ as the supporting electrolyte. Solutions were purged with argon and stirred prior to study. A blanket of argon was kept over the solutions for all experiments. Solutions were prepared immediately before measurements were to be taken. Scans were made at rate of 50 mV s^{-1} and then 100–1000 mV s^{-1}, increasing by 100 mV. The 1.5-mm glassy carbon working electrode was polished with a 1-μm diamond paste, rinsed with acetone, and then polished with 1/4-μm diamond paste. Prior to use, the working electrode was rinsed with acetone and then DCM. A platinum wire counter electrode was used along with a non-aqueous silver/silver chloride reference electrode.

5. Supplementary material

Crystallographic data (CIF files) for the structural analysis have been deposited with the Cambridge Crystallographic Data Centre, CCDC no. 209799. Copies of this information may be obtained free of charge from The Director, CCDC, 12 Union Road, Cambridge CB2 1EZ, UK (Fax: +44-1223-336033; e-mail: deposit@ccdc.cam.ac.uk or http://www.ccdc.cam.ac.uk).

Acknowledgements

AO'C was supported in part by the Academic Research Committee at Lafayette College through an EXCEL scholarship. AO'C and CN would like to thank the donors of the Petroleum Research Fund, administered by the American Chemical Society, for partial support of this research and the Kresge Foundation for the purchase of the JEOL Eclipse 400 MHz NMR.

References

[1] K.-S. Gan, T.S.A. Hor, in: A. Togni, T. Hayashi (Eds.), Ferrocenes. From Homogeneous Catalysis to Material Science, VCH, New York, 1995 (Chapter 1).
[2] G. Bandoli, A. Dolmella, Coord. Chem. Rev. 209 (2000) 161.
[3] T.S.A. Hor, L.-T. Phang, J. Organomet. Chem. 373 (1989) 319.
[4] E. Stein, F.Y. Fujiwara, J. Organomet. Chem. 525 (1996) 31.
[5] (a) L. Lassová, H.K. Lee, T.S.A. Hor, J. Org. Chem. 63 (1998) 3538;
(b) L. Lassová, H.K. Lee, T.S.A. Hor, J. Mol. Catal. A 144 (1999) 397.

[6] R.T. Hembre, J.S. McQueen, V.W. Day, J. Am. Chem. Soc. 118 (1996) 798.
[7] (a) D.L. DuBois, C.W. Eigenbrot, Jr., A. Miedaner, J.C. Smart, C. Haltiwanger, Organometallics 5 (1986) 1405;
(b) C.E. Housecroft, S.M. Owen, P.R. Raithby, B.A.M. Shaykh, Organometallics 9 (1990) 1617;
(c) A. Greff, P. Diter, D. Guillaneux, H.B. Kagan, New J. Chem. 21 (1997) 1353.
[8] (a) B. Corain, B. Longato, G. Favero, D. Ajò, G. Pilloni, U. Russo, F.R. Kreissl, Inorg. Chim. Acta 157 (1989) 259;
(b) G. Pilloni, B. Longato, B. Corain, J. Organomet. Chem. 420 (1991) 57;
(c) A.E. Gerbase, E.J.S. Vichi, E. Stein, L. Amaral, A. Vasquez, M. Hörner, C. Maichle-Mössmer, Inorg. Chim. Acta 266 (1997) 19.
[9] (a) T.M. Miller, K.J. Ahmed, M.S. Wrighton, Inorg. Chem. 28 (1989) 2347;
(b) P. Zanello, G. Opromolla, G. Giorgi, G. Sasso, A. Togni, J. Organomet. Chem. 506 (1996) 61;
(c) D.S. Shephard, B.F.G. Johnson, A. Harrison, S. Parsons, S.P. Smidt, L.J. Yellowlees, D. Reed, J. Organomet. Chem. 563 (1998) 113.
[10] C. Nataro, A.N. Campbell, M.A. Ferguson, C.D. Incarvito, A.L. Rheingold, J. Organomet. Chem. 673 (2003) 47.
[11] S.T. Chacon, W.R. Cullen, M.I. Bruce, F.W.B. Einstein, R.H. Jones, A.C. Willis, Can. J. Chem. 65 (1990) 2001.
[12] R.J. Angelici, Acc. Chem. Res. 28 (1995) 51.
[13] (a) D. Braga, F. Grepioni, L.J. Farrugia, B.F.G. Johnson, J. Chem. Soc. Dalton Trans. (1994) 2911;
(b) M.R. Churchill, F.J. Hollander, J.P. Hutchinson, Inorg. Chem. 16 (1977) 2655.
[14] P.M. Van Calcar, M.M. Olmstead, A.L. Balch, Inorg. Chim. Acta 270 (1998) 28.
[15] D. Braga, F. Grepioni, E. Tedesco, P.J. Dyson, C.M. Martin, B.F.G. Johnson, Transit. Met. Chem. 20 (1995) 615.
[16] C. Muller, R. Bartsch, A. Fischer, P.G. Jones, J. Organomet. Chem. 453 (1993) C16.
[17] O. bin Shawkataly, K. Ramalingam, D.M. Ashari, H.-K. Fun, I.A. Razak, Z. Kristallogr, New Cryst. Struct. 213 (1998) 369.
[18] N. Camire, U.T. Muller-Westerhoff, W.E. Geiger, J. Organomet. Chem. 637–639 (2001) 823.
[19] The literature reports the potentials vs. Ag/AgCl which was corrected to ferrocene (Fc = 0.44 V vs. Ag/AgCl in DCM/0.1 M $[Bu_4N][PF_6]$) [20].
[20] G. Zerza, A. Cravino, H. Neugebauer, N.S. Sariciftci, R. Goméz, J.L. Segura, N. Martín, M. Svensson, M.R. Andersson, J. Phys. Chem. A 105 (2001) 4172.
[21] A.J. Downard, B.H. Robinson, J. Simpson, J. Organomet. Chem. 320 (1987) 363.
[22] J.E. Cyr, P.H. Reiger, Organometallics 10 (1991) 2153.
[23] D. Osella, J. Hanzlík, Inorg. Chim. Acta 213 (1993) 311.
[24] D. Wang, R.J. Angelici, J. Am. Chem. Soc. 118 (1996) 935.
[25] S.S. Kristjánsdóttir, J.R. Norton, in: A. Dedieu (Ed.), Transition Metal Hydrides: Recent Advances in Theory and Experiment, VCH, Weinheim, 1991 (Chapter 9).
[26] W.E. Geiger, N.G. Connelly, Adv. Organomet. Chem. 24 (1985) 87.
[27] C. Nataro, L.M. Thomas, R.J. Angelici, Inorg. Chem. 36 (1997) 6000.
[28] L.J. Farrugia, J. Appl. Cryst. 30 (1997) 565.